

# Fundamentals of ion mobility spectrometry

Valérie Gabelica,<sup>1</sup> Erik Marklund<sup>2</sup>

1. Univ. Bordeaux, INSERM, CNRS, Laboratoire Acides Nucléiques Régulations Naturelle et Artificielle (ARNA, U1212, UMR5320), IECB, 2 rue Robert Escarpit, 33607 Pessac, France.

E-mail: [v.gabelica@iecb.u-bordeaux.fr](mailto:v.gabelica@iecb.u-bordeaux.fr)

2. Department of Chemistry – BMC, Box 576, SE-751 23 Uppsala University, Sweden.

E-mail: [erik.marklund@kemi.uu.se](mailto:erik.marklund@kemi.uu.se)

## Abstract

Fundamental questions in ion mobility spectrometry have practical implications for analytical applications in general, and omics in particular, in three respects. (1) Understanding how ion mobility and collision cross section values depend on the collision gas, on the electric field and on temperature is crucial to ascertain their transferability across instrumental platforms. (2) Predicting collision cross section values for new analytes is necessary to exploit the full potential of ion mobility in discovery workflows. (3) Finally, understanding the fate of ion structures in the gas phase is essential to infer meaningful information on solution structures based on gas-phase ion mobility measurements. We will review here the most recent advances in ion mobility fundamentals, related to these three aspects.

## Introduction

Omics sciences require to separate, identify and quantify all compounds in a mixture. Ion mobility spectrometry (IMS), which drags analytes through a buffer gas using electric fields, is useful for separation science, but can also aid identification. We review here the fundamental principles behind using IMS for identification and structural characterization. Although theoretical foundations were laid decades ago [1,2], fundamental contributions have flourished in the last two years. We gathered contributions of prime importance for IMS, spanning from small molecules (lipidomics, metabolomics) to large multi-protein assemblies (structural proteomics and native mass spectrometry).

In IMS, the force exerted by an electric field on an analyte ion is exactly balanced by friction with the buffer gas, yielding a steady-state analyte velocity  $v_d$ . The ion mobility  $K$  (Eq. 1) is thus a measure of friction linked to an observable, the time  $t_d$  the ions take to traverse the length  $l$  of the mobility cell.

$$K = \frac{v_d}{E} = \frac{t_d}{lE} \quad (1)$$

$K$  depends on collision frequency, hence on the gas number density ( $N$ ), gas temperature ( $T$ ) and pressure ( $p$ ), so the reduced mobility  $K_0 = K.N/N_0 = K.(p/p_0)/(T/T_0)$  is better to compare different experiments (in standard conditions,  $N_0 = 2.687 \times 10^{25} \text{ m}^{-3}$ ,  $p_0 = 760 \text{ Torr}$ ,  $T_0 = 273.16 \text{ K}$ ). When  $v_d$  is small compared to the ion thermal velocity  $v_T$ ,  $K$  can be expressed as Eq. (2) [1].

$$K = \frac{3}{16} \sqrt{\frac{2\pi}{\mu k_B T} \frac{ze}{N} \frac{1}{\Omega}} \quad (2)$$

$\mu$  is the reduced mass of the ion–gas pair ( $\mu = mM/(m+M)$ , where  $m$  and  $M$  are the ion and gas-particle masses),  $k_B$  is the Boltzmann constant, and  $ze$  is the analyte charge.  $\Omega$ , often called the “collision cross section” (CCS), is the “momentum transfer collision integral”, that is, the momentum transfer between ion and gas particles averaged over all gas-ion relative thermal velocities.  $\Omega$  has the dimensions of a surface, is a property of the ion–gas pair, and also depends on  $T$  and  $E$  because those parameters influence the ion–gas collision velocities. The first section will review the effects of gas, field and temperature, which are crucial for accurate interpretation of the data and for understanding differences between instrumental setups.

IMS practitioners have three main ways to characterize the analytes:  $t_d$  (in practice, the arrival time at a detector,  $t_A$ ),  $K_0$ , and  $\Omega$ . Each of these values can aid identification of “*known knowns*” (molecules whose presence is anticipated by the researcher, by comparison with a measured database) or of “*known unknowns*” (compounds that are unknown to the researcher, but described in the literature, by comparison with a predicted database). However, only  $\Omega$  can aid the identification of “*unknown unknowns*”, by comparing values predicted from putative candidate structures (Figure 1). The fundamentals of CCS calculation will be covered in the second section. Finally, we highlight recent examples of how IMS measurements and modeling shed new light on one of the most fundamental questions of mass spectrometry: how the structure in the gas phase relates to that in solution.

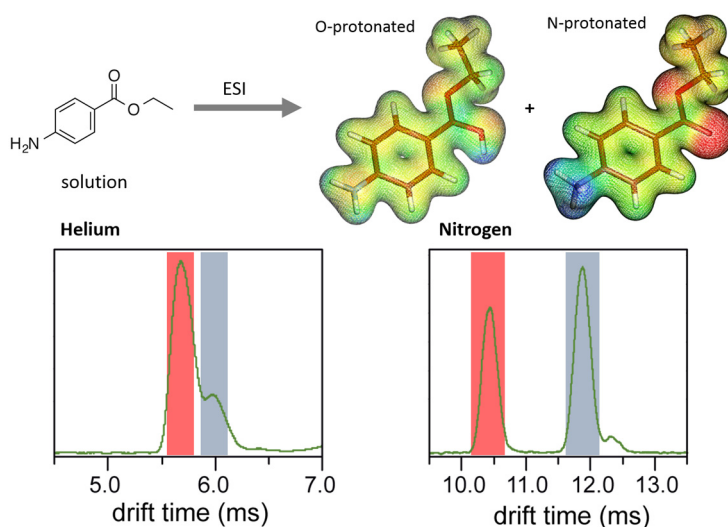


**Figure 1:** The O-protonated and N-protonated forms of benzocaine, produced simultaneously by electrospray in acetonitrile, separate differently in helium or nitrogen drift tube ion mobility (image courtesy of Kevin Pagel [10<sup>●●</sup>]).

### Effect of drift gas on collision cross sections

Early IMS for structural elucidation was carried out in drift tubes (DT) operated in helium, because calculations were easier. Using IMS for omics became possible with the introduction of commercial high-performance electrospray IMS mass spectrometers, usually operated in nitrogen. The first commercial IMS (the Synapt HDMS™, introduced by Waters in 2006)

operates with traveling wave (TW) IMS [3]. Because the electric field is not static in TWIMS, drift time is not commensurate to that of drift tubes. An empirical correlation was made to match arrival times based on helium drift-tube CCSs [4], and recently the  $t_d$  of peptides and proteins could be modeled at low wave velocities directly from  $K$  without calibration [5].

Experience however showed that TWIMS calibration is not universal: CCS values depend on the nature of the calibrant, which should have size, charge, and chemical class similar to the analytes (doing so results in an average deviation of  $< 2\%$  between  $^{TW}\Omega_{N_2 \rightarrow He}$  and  $^{DT}\Omega_{He}$  [6]). Similarly, native protein complexes should be used for structural proteomics [7]. However, Konermann's group recommends using denatured proteins even for native protein analytes, denatured proteins do not change CCS values when changing pre-IMS activation conditions [8]. Recently, the Robinson group also showed that soluble proteins are inappropriate calibrants for membrane proteins [9]. A hot question for TWIMS users is thus: "*What makes a calibrant suitable for my analytes?*"

Helium drift tube CCS values are often used to calibrate TWIMS instruments operated in nitrogen, so let's first discuss the effects of the drift gas on the CCS. Benzocaine will serve as textbook example for small molecules. In positive-mode electrospray, benzocaine exist in two tautomers (different proton location, but same conformation) [10<sup>●●</sup>]. They are readily separated by IMS in nitrogen, but overlap in helium (Figure 1). At 300K, interactions between the ions and the helium are akin to collisions with a hard sphere, hence the mobility difference is small. In contrast, nitrogen is polarizable, and interacts more strongly with the more polar tautomer [11]. The proportionality factor between helium and nitrogen CCS values thus depends on the chemical nature (here, charge location) of the analyte, and this effect is strongest for small ions.

Recent simulations of how  $\Omega$  depends on the gas temperature and identity highlight how the trends depend on the ion charge [12] and shape [13<sup>●●</sup>] (Figure 2).  $\Omega$  increases when the temperature decreases, because long-range interactions become more dominant at reduced  $v_T$ . At high temperature,  $\Omega$  approaches the hard-sphere limit. The difference is due to the gas-particle radius, and correlates with ion size and shape [13<sup>●●</sup>]. However at lower temperatures, *including room temperature*, the difference between He and N<sub>2</sub> is further influenced by long-range interactions, which depend on the gas polarizability, ion net charge [12] (Figure 2, top), and exact charge localization as illustrated by the benzocaine example [10<sup>●●</sup>] (the effect however

seems negligible for proteins [14]). Finally, the ion shape also matters (Figure 2, bottom). In the case of proteins, denatured conformations expose more residues than globular ones, and this increases the interactions with the gas.

In summary, the ratio between  $\Omega_{N_2}$  and  $\Omega_{He}$  depends on (i) the temperature, (ii) the ion charge, (iii) the charge localization, (iv) ion size and (v) ion shape. Yet, helium-to-nitrogen CCS conversion do not suffice to explain all compound-class effects on empirical TWIMS calibrations: even when calibrating TWIMS with drift tube CCS values measured in nitrogen, compound class still matters [9,15]. Differences in field heating regimes, combined with the temperature dependence of nitrogen CCSs, could explain this phenomenon.

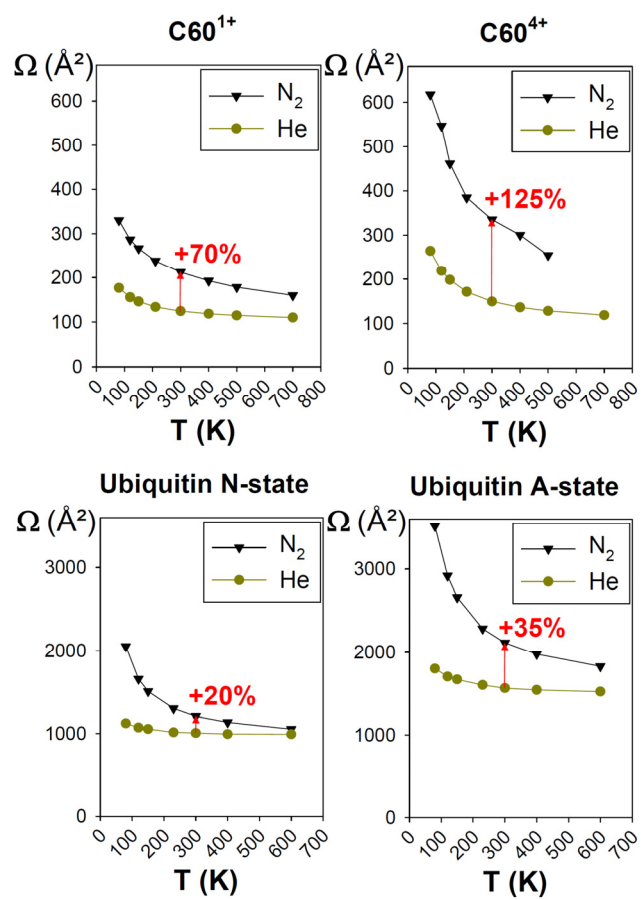


**Figure 2:** Calculated temperature dependence of CCSs in N<sub>2</sub> and He (top) for C<sub>60</sub> at two different charge states, using the trajectory model [12], and (bottom) for ubiquitin in two different conformations (N-state is native, A-state is less compact), using the projection superposition approximation [13<sup>••</sup>].

## Are we measuring ion mobility at the low-field limit?

Understanding the  $E/N$  effect is crucial to determine whether  $K_0$  or  $\Omega$  values can be compared across different platforms, the confidence with which databases can be shared, and the expected error or bias. Equations (1-2) are usually presented without questioning their validity. However, the ion mobility  $K$  is not a constant, because it depends on the  $E/N$  ratio (expressed in Townsends;  $1 \text{ Td} = 10^{-21} \text{ V.m}^2$ ). The low-field limit means that  $E/N$  is small enough so that  $K$  is independent of  $E/N$ . Importantly, Eq. (2) is valid only in the low-field limit. The value of the maximum electric field at which the instrument can operate without affecting the ion mobility in a noticeable way depends on the ion-gas pair. For atomic ions in noble gases, the low-field limit is of the order of 10 Td [16] but recently,  $E/N$  effects for polyatomic ions were reported below 4 Td [17,18]. Such ongoing research matters, because typical  $E/N$  values of modern high-performance IMS instruments may well be outside of the low-field limit (Table 1).

A key recent contribution is the momentum transfer theory [19,20]\*\*, which improves Equation (2) for non-zero fields and for ions significantly heavier than the buffer gas (thus, adapted to omics applications). Equation (2) is valid only at electric fields weak enough so that  $v_D$  is small compared to  $v_T$  at zero field (Eq. 3).

$$v_T = \sqrt{\frac{8k_B T}{\pi \mu}} \quad (3)$$

For  $T = 300 \text{ K}$  and  $m = 200$ ,  $v_T$  is 1239 m/s in helium and 495 m/s in dinitrogen. In Table 1, we see that in traveling wave IMS,  $v_D$  becomes dangerously close to  $v_T$ , and thus Equation (2) is not necessarily valid. The magnitude of the ensuing errors remains to be determined.

Moreover, working above the low-field limit means that field heating could change the effective temperature of the ions, resulting in measurable fragmentation [21,22] or isomerization [23] as shown for ions of 200-300 Da in TWIMS. In the previous section, we saw that (1) nitrogen CCSs vary with the temperature in the 300-500K range, and that (2) analyte chemistry influence the  $T$ -dependency. Class-dependent calibration problems in TWIMS could thus also come from ion temperatures in TWIMS differing from the calibrant DTIMS temperatures. In summary, DT and TW experiments will transpose well only if analytes and calibrant CCS values have the same temperature dependency in nitrogen. This condition is more likely to be met if calibrant and

analyte are similar in charge, charge localization (depending on analyte size), size and shape. We hope further studies, in particular with temperature-dependent drift tubes [24], will help test our proposal.

**Table 1. Estimates of typical operating parameters for contemporary commercial instruments.**

<b>Instrument and manufacturer</b>	<b>Operation principle</b>	<b><math>p</math> (Torr)</b>	<b><math>E</math> (V/cm)</b>	<b>Typical <math>E/N</math> (Td)</b>	<b>Typical <math>v_D</math> (m/s)</b>
6560 IMS-Q-TOF, Agilent Technologies	Drift tube	4	9.5-20	7-15 [25]	10-80
Synapt HDMS, Waters	TWIMS	0.4	21 (maximum axial field at wave height = 10 V) [26]	$\leq 160$	200-600 [21]
Synapt G2, G2-S and G2Si HDMS, Waters	TWIMS	2	100 (maximum axial field at wave height = 40 V)	$\leq 155$	200-300 [22]
TIMS-TOF, Bruker	TWIMS	2	30-55	45-85	120-170* [27]
IMS-TOF, Tofwerk	Drift tube	570- 788	$\sim 400$	1-2 [28]	$\sim 5$

\* Gas velocity; in TIMS the ion is static.

## Structural interpretation based on collision cross sections

Since the information contained in the CCS alone is insufficient to uniquely define the analyte structure, molecular modelling plays an important role in structural interpretation of IMS data, i.e., for unknown unknowns. The approach, conceived almost a century ago [29], is to calculate CCS values for candidate structure models and compare them with experimentally derived CCS values. Several methods have emerged (Table 2 and Figure 3), and the majority shoots buffer-gas probes toward a (static) analyte in a Monte-Carlo integration of the collision integral. Their main differences stem from what trade-offs between speed and physical rigor follow from their underlying assumptions.

The Trajectory Method (TM) treats long- and short-range interactions (we saw above that this is necessary for small molecules in nitrogen) and the  $v_T$  distribution explicitly [30]. The numerous force evaluations for each trajectory, combined with the vast integration domain, makes TM extremely time consuming (Table 2) [31<sup>•</sup>,32,33]. A solution is to replace trajectory calculations by a local collision probability approximation (LCPA) [34]. Adaptation for molecular buffer gasses [35-38] strengthens TM's fundamental position for CCS calculation. TM in its canonical form assumes elastic collisions, which is not a fully valid assumption for molecular buffer gases, and extension to accommodate inelastic scattering is an important enhancement [39].

For larger analytes, long-range interactions become less influential [12,35], allowing for further approximations. The Elastic Hard Sphere Scattering (EHSS) method [40-42] disregards long-range interactions, considering only hard-sphere collisions. The Projection Approximation (PA) completely ignores scattering, assuming the CCS to be the analyte's rotationally averaged projected area (taking the buffer-gas particle radius into account) [29], and the PA CCS is thus an (inverse) metric of the analyte's self-occlusion [43]. These methods require no integration of individual probe trajectories and are considerably faster than TM [31<sup>••</sup>,32,33], yet can surprisingly give results within a few percent of TM values [14,31<sup>••</sup>,32], either through calibration [31<sup>••</sup>] or by their own accord if the effects of surface roughness average out. Domain-decomposition schemes give PA a performance boost for large structures [31<sup>••</sup>,44], and future gains might be made by exploiting mathematical properties of projected areas [43]. Similar enhancements are conceivable also for the more rigorous methods, but remain to be implemented. Omission of long-range interactions make EHSS and PA invariant to temperature,

although temperature-dependent atom radii can circumvent this problem to some degree [32,45]. PA lends itself for analysis of non-atomistic structures, including bead models [46] and electron-densities [31<sup>●●</sup>,47]. Building on PA, Projected Superposition Approximation (PSA) employs a mean-field approximation for scattering, based on the surface characteristics of the analyte, and approximates long-range interactions via distance- and temperature-dependent collision probability [32]. PSA is more able than PA to handle non-globular structures, at the cost of four orders of magnitude in throughput (Table 2).

Machine learning using various molecular descriptors offers a radically different alternative to calculation of the (approximated) collision integral. For small molecules this yields accurate CCSs for approximately 90% of tested analytes [48<sup>●●</sup>,49<sup>●●</sup>], outperforming TM [49<sup>●●</sup>]. Some descriptors are computationally expensive, but less so than TM calculations [48<sup>●●</sup>], and omitting geometric properties drastically improves throughput [49<sup>●●</sup>]. This approach is not yet available for protein-sized analytes, but could be a powerful alternative if such parameterization is possible.

**Table 2. Methods for calculating CCSs of a given structure, their performance, and available implementations. Performance is given as the approximate time for computing the CCS of a protein structure to a statistical error of 1%.**

Method	Computing time (s)	Available implementations
TM	63 100 [31]	Mobcal, ImOS* [39], Collidoscope [50]
EHSS	1670 [31]	Mobcal, ImOS*
PA	0.07 [31]	Mobcal, ImOS, Sigma <sup>†</sup> [51], Impact [31 <sup>●●</sup> ], CCSCalc [52]
PSA	663 [32]	-

\*) ImOS additionally implements diffuse scattering versions of TM and EHSS – DTM and DHSS – which extends the physical model to take non-elastic collisions into account.

†) Implements a mass-dependent scaling factor to take into account the collective long-range interactions from many atoms.

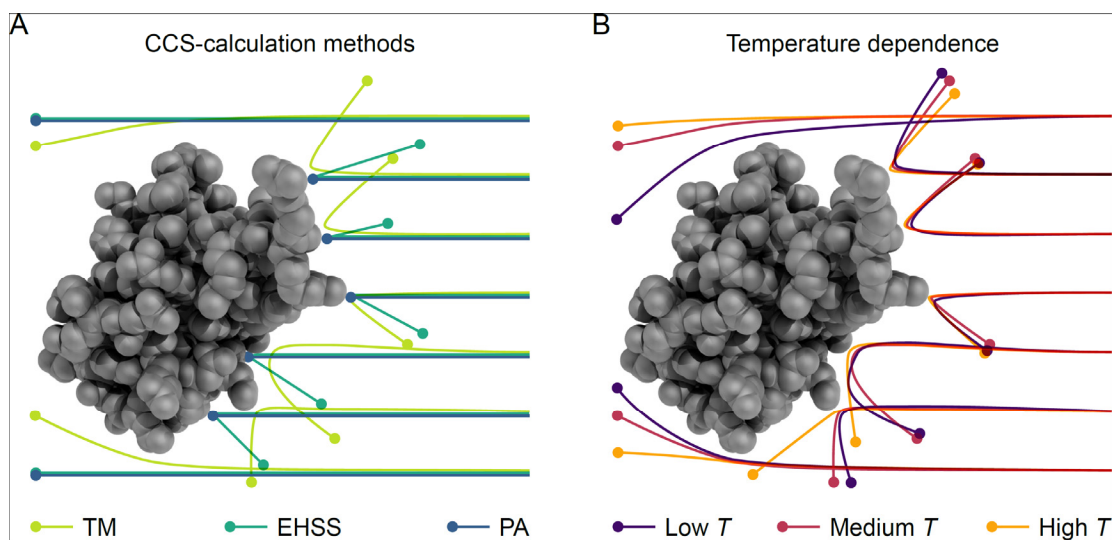


**Figure 3:** **A)** The principal operation and differences between the main classes of CCS calculation methods. TM traces the probe particles' trajectories, whereas EHSS and PA only regards direct contact between probes and analyte. The EHSS considers (multiple) scattering after initial collision, whereas PA only differentiates between hits and misses, and estimates CCSs from the fraction of hits. **B)** At higher temperatures, the momentum transfer between buffer gas and analyte effectively decreases. This is easily seen for low-temperature collisions, which are deflected more as they pass the analyte.

### Do gas-phase ion structures reflect the solution phase ones?

The gas phase structure can differ from the solution (1) because of the ionization, and (2) because of a different balance of interactions. In physical chemistry terms, this is represented by different potential energy surfaces (PES) for the solution and the gas phase [53]. With low internal energy (i.e. just enough for desolvation and declustering) one hopes to trap conformations that have kept some memory of the solution ones [53]. Large proteins and protein complexes are likely to preserve salt bridges [54], but smaller analytes can retain structural elements as well. For example, IMS was successfully used to study the solution biophysics of cis-trans isomerization of polyproline [55,56<sup>•</sup>]. Even small pentapeptides can adopt kinetically trapped conformations in the gas phase [57], so the internal energy dependence of gas-phase conformations can be relevant proteomics workflows as well. The experiment time scales are a

determining factor for the survival of native-like states. The typical IMS experiment take micro- to milliseconds, with little interconversion between distinguishable protein conformers [58], whereas for longer times the populations of extended conformations increase [59].

Still, to our opinion, representing a single gas-phase PES is still an oversimplification, because there are as many co-existing potential energy surfaces as there are ways to locate the charges. We have seen that for small molecules, a single analyte in solution can give two mobility peaks corresponding to two possible protonation sites in the gas phase. This is an important fundamental insight for metabolomics interpretation, and a warning that the number of “features” observed in IM-MS is not necessary equal to the number of distinct compounds in the sample. For larger, multiply charged ions, it would be further useful to distinguish charge macrostates (total charge) from charge microstates (a particular distribution of charge locations). In addition, molecular flexibility favors proton migrations in the gas phase, also at room temperature, as shown for protein polycations [60<sup>●</sup>], glycan monoanions [61] and oligonucleotide polyanions [62]. In turn, proton migration allows the ion to explore different microstates with other conformations. This tremendously complicates the molecular modelling of gas-phase structural ensembles. Further complicating the assignment based on structural modeling, fast interconverting structures have drift times corresponding to their abundance-weighted average CCSs, not to CCSs of individual conformations [61]. Cations ( $\text{Na}^+$ ,  $\text{Ca}^{2+}$ , ...) are less mobile at room temperature, thereby freezing conformations. This helps for some analytical applications, for example in carbohydrate analysis [63].

As the analytes become larger (e.g., proteins), the width of the charge-state and CCS distributions are generally correlated with flexibility and disorder [64-66]. Broader-than-diffusion ion mobility peaks result from flexible structures rearranging in a myriad different ways and coexisting without interconverting after transfer to the gas phase, to self-solvate their charges [67<sup>●</sup>]. Broad peaks obtained from native proteins [58] indicate that this phenomenon is not restricted to intrinsically disordered structures and warrants attention. This is purely a gas phase process, as demonstrated by IMS on low-charge state proteins produced by neutralization of high charge-state ones [68,69]. However, collision-induced unfolding allows to differentiate conformational ensembles from the way they change with internal energy [70]. When the total charge repulsion overcomes the intramolecular binding forces including salt bridges (akin to an

intramolecular Rayleigh limit), large flexible molecules elongate to conformations much more extended than in solution [71,72]. For these reasons, intrinsically disordered proteins adopt both more compact and more extended (depending on the charge state) conformations in the gas-phase compared to the solution [73<sup>••</sup>]. Finally, note that compact conformations does not necessarily mean that the solution structure is preserved, because at low charge states, collision-induced rearrangements can lead to compaction as well [74].

## Concluding remarks

Over recent years IMS has boosted fundamental studies on ion structures in the gas phase, and their relationship with the electrospray process (charging and mode of ejection from the droplets) and with internal energy. A picture emerges, in which the relationship between solution and gas-phase structure is not always straightforward, but we anticipate that this lively area of research will soon help us rationalize many puzzling observations and deduce gas-phase structural rules that will in the future nourish routine application of ion mobility in omics studies.

Reflecting the complexity and the dependence on experimental detail, we propose to go beyond the reporting of single CCS. Measurement in multiple buffer gasses [13<sup>••</sup>], at different temperatures, or with different electric fields (for example, using Field Asymmetric Ion Mobility Spectrometry (FAIMS)), once the fundamentals will be understood, will paint a more complete picture of the analyte. The differences in CCS values, instead of being an annoyance for inter-instrument comparisons, would rather provide additional information for identification.

On the modelling side, we would welcome development of force fields better suited for MD under gas-phase conditions, possible including polarizability, and further development of methods for dynamic proton-transfer; both of which would enable more accurate studies of fundamental aspects of IMS and MS. For CCS calculations, we would like to see further exploration of when the more approximate methods can be used in place of TM, their proper parameterization, and how they can be calibrated. The throughput difference between TM and PA is about a million-fold, with clear implications on the number of structure models that can be tested, which translates to the strength of the interpretations made. Inelastic collisions and the

impact of gas-phase dynamics on the CCSs are also pertinent aspects, where CCS calculations and MD simulations can combine.

As this review has outlined, many fundamental questions have been answered over recent years. Many remain however, and the coming years have potential to bring great progress to IMS for omics applications.

**Acknowledgements.** We thank Kevin Pagel for providing the illustrations for Figure 1. This work was funded by the European Research Council (ERC-2013-CoG-616551-DNAFOLDIMS to VG) and by the EU H2020 program (Marie Skłodowska Curie INCA fellowship to EM).

## References

1. Revercomb HE, Mason EA: **Theory of plasma chromatography/gaseous electrophoresis - a review.** *Anal. Chem.* 1975, **47**:970-983.
2. Mason EA, McDaniel W: *Transport properties of ions in gases*: Wiley; 1988.
3. Giles K, Pringle SD, Worthington KR, Little D, Wildgoose JL, Bateman RH: **Applications of a travelling wave-based radio-frequency only stacked ring ion guide.** *Rapid Commun. Mass Spectrom.* 2004, **18**:2401-2414.
4. Ruotolo BT, Benesch JL, Sandercock AM, Hyung SJ, Robinson CV: **Ion mobility-mass spectrometry analysis of large protein complexes.** *Nat. Protoc.* 2008, **3**:1139-1152.
5. Mortensen DN, Susa AC, Williams ER: **Collisional Cross-Sections with T-Wave Ion Mobility Spectrometry without Experimental Calibration.** *J. Am. Soc. Mass Spectrom.* 2017, **28**:1282-1292.
6. Bush MF, Campuzano ID, Robinson CV: **Ion mobility mass spectrometry of peptide ions: effects of drift gas and calibration strategies.** *Anal. Chem.* 2012, **84**:7124-7130.
7. Bush MF, Hall Z, Giles K, Hoyes J, Robinson CV, Ruotolo BT: **Collision cross sections of proteins and their complexes: a calibration framework and database for gas-phase structural biology.** *Anal. Chem.* 2010, **82**:9557-9565.

8. Sun Y, Vahidi S, Sowole MA, Konermann L: **Protein Structural Studies by Traveling Wave Ion Mobility Spectrometry: A Critical Look at Electrospray Sources and Calibration Issues.** *J. Am. Soc. Mass Spectrom.* 2016, **27**:31-40.
9. Allison TM, Landreh M, Benesch JL, Robinson CV: **Low Charge and Reduced Mobility of Membrane Protein Complexes Has Implications for Calibration of Collision Cross Section Measurements.** *Anal. Chem.* 2016, **88**:5879-5884.
10. ●● Warnke S, Seo J, Boschmans J, Sobott F, Scrivens JH, Bleiholder C, Bowers MT, Gewinner S, Schollkopf W, Pagel K, et al.: **Protomers of benzocaine: solvent and permittivity dependence.** *J. Am. Chem. Soc.* 2015, **137**:4236-4242.

In this textbook example, the authors show that depending on the electrospray solvent, two protomers are produced starting from benzocaine, that they can be separated by ion mobility spectrometry in nitrogen (although not in helium), and structurally identified through gas-phase infrared spectroscopy.

11. Boschmans J, Jacobs S, Williams JP, Palmer M, Richardson K, Giles K, Laphorn C, Herrebout WA, Lemiere F, Sobott F: **Combining density functional theory (DFT) and collision cross-section (CCS) calculations to analyze the gas-phase behaviour of small molecules and their protonation site isomers.** *Analyst* 2016, **141**:4044-4054.
12. Young MN, Bleiholder C: **Molecular Structures and Momentum Transfer Cross Sections: The Influence of the Analyte Charge Distribution.** *J. Am. Soc. Mass Spectrom.* 2017, **28**:619-627.
13. ●● Bleiholder C, Johnson NR, Contreras S, Wyttenbach T, Bowers MT: **Molecular Structures and Ion Mobility Cross Sections: Analysis of the Effects of He and N<sub>2</sub> Buffer Gas.** *Anal. Chem.* 2015, **87**:7196-7203.

The reader will find here a thorough fundamental discussion of the effect of the collision gas on the collision cross section of molecules with a variety of size and shape.

14. Shrivastav V, Nahin M, Hogan CJ, Larriba-Andaluz C: **Benchmark Comparison for a Multi-Processing Ion Mobility Calculator in the Free Molecular Regime.** *J. Am. Soc. Mass Spectrom.* 2017, **28**:1540-1551.

15. Hines KM, May JC, McLean JA, Xu L: **Evaluation of Collision Cross Section Calibrants for Structural Analysis of Lipids by Traveling Wave Ion Mobility-Mass Spectrometry.** *Anal. Chem.* 2016, **88**:7329-7336.
16. Shvartsburg AA: *Differential ion mobility spectrometry. Nonlinear ion transport and fundamentals of FAIMS.* Boca Raton: CRC Press; 2009.
17. Hauck BC, Siems WF, Harden CS, McHugh VM, Hill HH, Jr.: ***E/N* effects on  $K_0$  values revealed by high precision measurements under low field conditions.** *Rev. Sci. Instrum.* 2016, **87**:075104.
18. Hauck BC, Siems WF, Harden CS, McHugh VM, Hill HH, Jr.: **Determination of *E/N* Influence on  $K_0$  Values within the Low Field Region of Ion Mobility Spectrometry.** *J. Phys. Chem. A* 2017, **121**:2274-2281.
19. Siems WF, Viehland LA, Hill HH, Jr.: **Improved momentum-transfer theory for ion mobility. 1. Derivation of the fundamental equation.** *Anal. Chem.* 2012, **84**:9782-9791.
20. Siems WF, Viehland LA, Hill HH: **Correcting the fundamental ion mobility equation for field effects.** *Analyst* 2016, **141**:6396-6407.
21. Morsa D, Gabelica V, De Pauw E: **Effective Temperature of Ions in Traveling Wave Ion Mobility Spectrometry.** *Anal. Chem.* 2011, **83**:5775-5782.
22. Morsa D, Gabelica V, De Pauw E: **Fragmentation and Isomerization Due to Field Heating in Traveling Wave Ion Mobility Spectrometry.** *J. Am. Soc. Mass Spectrom.* 2014, **25**:1384-1393.
23. Poyer S, Comby-Zerbino C, Choi CM, MacAleese L, Deo C, Bogliotti N, Xie J, Salpin JY, Dugourd P, Chirof F: **Conformational Dynamics in Ion Mobility Data.** *Anal. Chem.* 2017, **89**:4230-4237.
24. Ujma J, Giles K, Morris M, Barran PE: **New High Resolution Ion Mobility Mass Spectrometer Capable of Measurements of Collision Cross Sections from 150 to 520 K.** *Anal. Chem.* 2016, **88**:9469-9478.
25. May JC, Goodwin CR, Lareau NM, Leaptrot KL, Morris CB, Kurulugama RT, Mordehai A, Klein C, Barry W, Darland E, et al.: **Conformational ordering of biomolecules in the gas**

**phase: nitrogen collision cross sections measured on a prototype high resolution drift tube ion mobility-mass spectrometer.** *Anal. Chem.* 2014, **86**:2107-2116.

26. Giles K, Wildgoose JL, Langridge DJ, Campuzano I: **A method for direct measurement of ion mobilities using a travelling wave ion guide.** *Int. J. Mass Spectrom.* 2010, **298**:10-16.
27. Silveira JA, Michelmann K, Ridgeway ME, Park MA: **Fundamentals of Trapped Ion Mobility Spectrometry Part II: Fluid Dynamics.** *J. Am. Soc. Mass Spectrom.* 2016, **27**:585-595.
28. Groessl M, Graf S, Knochenmuss R: **High resolution ion mobility-mass spectrometry for separation and identification of isomeric lipids.** *Analyst* 2015, **140**:6904-6911.
29. Mack E: **Average cross-sectional areas of molecules by gaseous diffusion methods.** *J. Am. Chem. Soc.* 1925, **47**:2468-2482.
30. Mesleh MF, Hunter JM, Shvartsburg AA, Schatz GC, Jarrold MF: **Structural information from ion mobility measurements: Effects of the long-range potential.** *J. Phys. Chem.* 1996, **100**:16082-16086.
31. ●● Marklund EG, Degiacomi MT, Robinson CV, Baldwin AJ, Benesch JLP: **Collision Cross Sections for Structural Proteomics.** *Structure* 2015, **23**:791-799.  
  
Presents a highly optimized PA CCS calculator that reproduces TM calculations within 1% error, and applies it to the entire Protein Data Bank in order to charter the known structural proteome from an IMS point of view.
32. Bleiholder C, Wyttenbach T, Bowers MT: **A novel projection approximation algorithm for the fast and accurate computation of molecular collision cross sections (I). Method.** *Int. J. Mass Spectrom.* 2011, **308**:1-10.
33. D'Atri V, Porrini M, Rosu F, Gabelica V: **Linking molecular models with ion mobility experiments. Illustration with a rigid nucleic acid structure.** *J. Mass Spectrom.* 2015, **50**:711-726.
34. Bleiholder C: **A local collision probability approximation for predicting momentum transfer cross sections.** *Analyst* 2015, **140**:6804-6813.

35. Kim H, Kim HI, Johnson PV, Beegle LW, Beauchamp JL, Goddard WA, Kanik I: **Experimental and theoretical investigation into the correlation between mass and ion mobility for choline and other ammonium cations in N<sub>2</sub>.** *Anal. Chem.* 2008, **80**:1928-1936.
36. Takaya K, Kaneko T, Tanuma H, Nishide T, Sugiyama H, Nakano N, Nagashima H, Seto Y: **Model calculation for ion mobility in air using the MOBCAL program.** *Int. J. Ion Mobil. Spectrom.* 2016, **19**:227-232.
37. Campuzano I, Bush MF, Robinson CV, Beaumont C, Richardson K, Kim H, Kim HI: **Structural Characterization of Drug-like Compounds by Ion Mobility Mass Spectrometry: Comparison of Theoretical and Experimentally Derived Nitrogen Collision Cross Sections.** *Anal. Chem.* 2012, **84**:1026-1033.
38. Kim HI, Kim H, Pang ES, Ryu EK, Beegle LW, Loo JA, Goddard WA, Kanik I: **Structural Characterization of Unsaturated Phosphatidylcholines Using Traveling Wave Ion Mobility Spectrometry.** *Anal. Chem.* 2009, **81**:8289-8297.
39. Larriba C, Hogan CJ: **Free molecular collision cross section calculation methods for nanoparticles and complex ions with energy accommodation.** *J. Comput. Phys.* 2013, **251**:344-363.
40. Shvartsburg AA, Jarrold MF: **An exact hard-spheres scattering model for the mobilities of polyatomic ions.** *Chem. Phys. Lett.* 1996, **261**:86-91.
41. Shvartsburg AA, Liu B, Jarrold MF, Ho KM: **Modeling ionic mobilities by scattering on electronic density isosurfaces: Application to silicon cluster anions.** *J. Chem. Phys.* 2000, **112**:4517-4526.
42. Alexeev Y, Fedorov DG, Shvartsburg AA: **Effective Ion Mobility Calculations for Macromolecules by Scattering on Electron Clouds.** *J. Phys. Chem. A* 2014, **118**:6763-6772.
43. Marklund EG: **Molecular self-occlusion as a means for accelerating collision cross-section calculations.** *Int. J. Mass Spectrom.* 2015, **386**:54-55.
44. Paizs B: **A divide-and-conquer approach to compute collision cross sections in the projection approximation method.** *Int. J. Mass Spectrom.* 2015, **378**:360-363.

45. Wytttenbach T, von Helden G, Batka JJ, Carlat D, Bowers MT: **Effect of the long-range potential on ion mobility measurements.** *J. Am. Soc. Mass Spectrom.* 1997, **8**:275-282.
46. Politis A, Park AY, Hall Z, Ruotolo BT, Robinson CV: **Integrative Modelling Coupled with Ion Mobility Mass Spectrometry Reveals Structural Features of the Clamp Loader in Complex with Single-Stranded DNA Binding Protein.** *J. Mol. Biol.* 2013, **425**:4790-4801.
47. Degiacomi MT, Benesch JLP: **EM boolean AND IM: software for relating ion mobility mass spectrometry and electron microscopy data.** *Analyst* 2016, **141**:70-75.
48. ●● Gonzales GB, Smaghe G, Coelus S, Adriaenssens D, De Winter K, Desmet T, Raes K, Van Camp J: **Collision cross section prediction of deprotonated phenolics in a travelling-wave ion mobility spectrometer using molecular descriptors and chemometrics.** *Anal. Chim. Acta* 2016, **924**:68-76.

Presents a fast machine-learning approach to predict CCS for small molecules.

49. ●● Zhou Z, Shen X, Tu J, Zhu Z-J: **Large-Scale Prediction of Collision Cross-Section Values for Metabolites in Ion Mobility-Mass Spectrometry.** *Anal. Chem.* 2016, **88**:11084-11091.

The CCS values of a metabolomics database are predicted by machine-learning, and shown to outperform CCS values calculated with TM. The predicted database is freely available.

50. Ewing SA, Donor MT, Wilson JW, Prell JS: **Collidoscope: An Improved Tool for Computing Collisional Cross-Sections with the Trajectory Method.** *J. Am. Soc. Mass Spectrom.* 2017, **28**:587-596.
51. Von Helden G, Hsu MT, Gotts N, Bowers MT: **Carbon Cluster Cations with up to 84 Atoms - Structures, Formation Mechanism, and Reactivity.** *J. Phys. Chem.* 1993, **97**:8182-8192.
52. Williams JP, Lough JA, Campuzano I, Richardson K, Sadler PJ: **Use of ion mobility mass spectrometry and a collision cross-section algorithm to study an organometallic ruthenium anticancer complex and its adducts with a DNA oligonucleotide.** *Rapid Commun. Mass Spectrom.* 2009, **23**:3563-3569.

53. Clemmer DE, Russell DH, Williams ER: **Characterizing the Conformationome: Toward a Structural Understanding of the Proteome.** *Acc. Chem. Res.* 2017, **50**:556-560.
54. Loo RR, Loo JA: **Salt Bridge Rearrangement (SaBRe) Explains the Dissociation Behavior of Noncovalent Complexes.** *J. Am. Soc. Mass Spectrom.* 2016, **27**:975-990.
55. Shi L, Holliday AE, Shi H, Zhu F, Ewing MA, Russell DH, Clemmer DE: **Characterizing intermediates along the transition from polyproline I to polyproline II using ion mobility spectrometry-mass spectrometry.** *J. Am. Chem. Soc.* 2014, **136**:12702-12711.
56. • Shi L, Holliday AE, Bohrer BC, Kim D, Servage KA, Russell DH, Clemmer DE: **"Wet" Versus "Dry" Folding of Polyproline.** *J. Am. Soc. Mass Spectrom.* 2016, **27**:1037-1047.
- Up to eight different folding states of polyproline-13 can be separated by ion mobility spectrometry, and it is shown that for cis-trans proline isomerization, gas-phase conformational changes bear resemblance to solution-phase ones.
57. Voronina L, Masson A, Kamrath M, Schubert F, Clemmer D, Baldauf C, Rizzo T: **Conformations of Prolyl-Peptide Bonds in the Bradykinin 1-5 Fragment in Solution and in the Gas Phase.** *J. Am. Chem. Soc.* 2016, **138**:9224-9233.
58. Koeniger SL, Merenbloom SI, Clemmer DE: **Evidence for Many Resolvable Structures within Conformation Types of Electrosprayed Ubiquitin Ions.** *J. Phys. Chem. B* 2006, **110**:7017-7021.
59. Liu FC, Kirk SR, Bleiholder C: **On the structural denaturation of biological analytes in trapped ion mobility spectrometry - mass spectrometry.** *Analyst* 2016, **141**:3722-3730.
60. • Li J, Lyu W, Rossetti G, Konijnenberg A, Natalello A, Ippoliti E, Orozco M, Sobott F, Grandori R, Carloni P: **Proton Dynamics in Protein Mass Spectrometry.** *J. Phys. Chem. Lett.* 2017, **8**:1105-1112.

The authors show through high-level quantum mechanics/molecular dynamics simulations, that peptides and proteins bear mobile protons also at room temperature, enabling conformational changes that influence the collision cross sections.

61. Struwe WB, Baldauf C, Hofmann J, Rudd PM, Pagel K: **Ion mobility separation of deprotonated oligosaccharide isomers – evidence for gas-phase charge migration.** *Chem. Commun.* 2016, **52**:12353-12356.
62. Arcella A, Dreyer J, Ippoliti E, Ivani I, Portella G, Gabelica V, Carloni P, Orozco M: **Structure and dynamics of oligonucleotides in the gas phase.** *Angew. Chem. Int. Ed.* 2015, **54**:467-471.
63. Huang Y, Dodds ED: **Ion-neutral collisional cross sections of carbohydrate isomers as divalent cation adducts and their electron transfer products.** *Analyst* 2015, **140**:6912-6921.
64. Beveridge R, Phillips AS, Denbigh L, Saleem HM, MacPhee CE, Barran PE: **Relating gas phase to solution conformations: Lessons from disordered proteins.** *Proteomics* 2015, **15**:2872-2883.
65. Li J, Santambrogio C, Brocca S, Rossetti G, Carloni P, Grandori R: **Conformational effects in protein electrospray-ionization mass spectrometry.** *Mass Spectrom. Rev.* 2016, **105**:111-122.
66. D'Urzo A, Konijnenberg A, Rossetti G, Habchi J, Li J, Carloni P, Sobott F, Longhi S, Grandori R: **Molecular basis for structural heterogeneity of an intrinsically disordered protein bound to a partner by combined ESI-IM-MS and modeling.** *J. Am. Soc. Mass Spectrom.* 2015, **26**:472-481.
67. • Porrini M, Rosu F, Rabin C, Darre L, Gomez H, Orozco M, Gabelica V: **Compaction of Duplex Nucleic Acids upon Native Electrospray Mass Spectrometry.** *ACS Cent. Sci.* 2017, **3**:454-461.

Duplex DNA is a cautionary example where, at the charge states obtained from electrospray physiological ionic strength, the gas-phase structure is significantly more compact than the original double-helix in solution, due to the intramolecular formation of non-native hydrogen bonds between phosphate groups.

68. Laszlo KJ, Munger EB, Bush MF: **Folding of Protein Ions in the Gas Phase after Cation-to-Anion Proton-Transfer Reactions.** *J. Am. Chem. Soc.* 2016, **138**:9581-9588.

69. Jhingree JR, Bellina B, Pacholarz KJ, Barran PE: **Charge Mediated Compaction and Rearrangement of Gas-Phase Proteins: A Case Study Considering Two Proteins at Opposing Ends of the Structure-Disorder Continuum.** *J. Am. Soc. Mass Spectrom.* 2017, **28**:1450-1461.
70. Zhong Y, Han L, Ruotolo BT: **Collisional and Coulombic Unfolding of Gas-Phase Proteins: High Correlation to Their Domain Structures in Solution.** *Angew. Chem. Int. Ed.* 2014, **53**:9209-9212.
71. Warnke S, Hoffmann W, Seo J, De Genst E, von Helden G, Pagel K: **From Compact to String-The Role of Secondary and Tertiary Structure in Charge-Induced Unzipping of Gas-Phase Proteins.** *J. Am. Soc. Mass Spectrom.* 2017, **28**:638-646.
72. Gonzalez Florez AI, Mucha E, Ahn D-S, Gewinner S, Schöllkopf W, Pagel K, Von Helden G: **Charge-Induced Unzipping of Isolated Proteins to a Defined Secondary Structure.** *Angew. Chem. Int. Ed.* 2016, **55**:3295-3299.
73. ●● Borysik AJ, Kovacs D, Guharoy M, Tompa P: **Ensemble Methods Enable a New Definition for the Solution to Gas-Phase Transfer of Intrinsically Disordered Proteins.** *J. Am. Chem. Soc.* 2015, **137**:13807-13817.

Another cautionary tale on the differences between solution and gas-phase structures: intrinsically disordered proteins are shown to undergo a vast conformational space expansion in the absence of solvent to sample a conformational space 3–5 fold broader than in solution.

74. Bornschein RE, Niu S, Eschweiler J, Ruotolo BT: **Ion Mobility-Mass Spectrometry Reveals Highly-Compact Intermediates in the Collision Induced Dissociation of Charge-Reduced Protein Complexes** *J. Am. Soc. Mass Spectrom.* 2016, **27**:41-49.